Azeotropic binary solvent mixtures for preparation of organic single crystals

Please check the document version of this publication:

• A submitted manuscript is the version of the article upon submission and before peer-review. There can be important differences between the submitted version and the official published version of record. People interested in the research are advised to contact the author for the final version of the publication, or visit the DOI to the publisher's website.
• The final author version and the galley proof are versions of the publication after peer review.
• The final published version features the final layout of the paper including the volume, issue and page numbers.

Link to publication

Azeotropic Binary Solvent Mixtures for Preparation of Organic Single Crystals

By *Xiaoran Li,* B. K. Charlotte Kjellander, John E. Anthony, Cornelis W. M. Bastiaansen, Dirk J. Broer,* and *Gerwin H. Gelinck**

Here, a new approach is introduced to prepare large single crystals of π-conjugated organic molecules from solution. Utilizing the concept of azeotropism, single crystals of tri-isopropylsilylethynyl pentacene (TIPS-PEN) with dimensions up to millimeters are facilely self-assembled from homogeneous solutions comprising two solvents with opposing polarities and a positive azeotropic point. At solvent compositions close to the azeotropic point, an abrupt transition of morphology from polycrystalline thin-films to large single crystals is found. How to adjust the initial ratio of the binary solvents so that the change in solvent composition during evaporation favors the specific H-aggregation and promotes an efficient self-assembly of TIPS-PEN is explained. The charge-carrier (hole) mobilities are substantially enhanced by a factor of 4 from the morphology of thin-films to large single crystals used as active layer in field-effect transistors. Additionally, this approach is extended to other π–π stacked organic molecules to elucidate its broad applicability.

1. Introduction

The last two decades have witnessed great research interests in the optoelectronic properties of organic semiconductors (OSC), and tremendous progress in their application to devices such as organic field-effect transistors (OFETs).[1–4] Serious efforts are now being undertaken to commercialize devices based on OFETs into products, e.g., active matrix display backplanes[5] and radio frequency identification (RFID) tags.[6] Typical deposition methods[7–11] for OSC lead to the formation of polycrystalline thin-film domains. The presence of disorder and/or poor grain connectivity[12] can adversely affect charge transport in OFETs. More recently, to better understand the charge transport mechanisms in OFETs and reveal the performance limits of OSC, various types of micrometer or nanometer organic single crystals based on π-conjugated aromatic molecules have been extensively studied.[13–15] Single crystals can be grown by sublimation through the physical vapor transport, and many groups have explored this route.[13–20] Relatively few reports have appeared where solution processing methods are used to form organic single crystal transistors.[4,13] One encouraging method is the so-called solvent exchange.[21–24] In this method, a small volume of a solution containing the OSC molecules in a ''good'' solvent is dispensed into a large excess of a ''bad'' solvent. As a result of weakened/minimized interaction between the OSC solute and the bad solvent, single crystals are formed.[22] Although high-mobility transistors have been made with this method, it suffers from several drawbacks. It is a slow process. Solution growth of single crystals using such a solvent-exchange method typically can take hours to days in a closed container, depending on how slowly the bad solvent needs to be driven off.[21,23] Furthermore, after the injection of a minimum volume of the good solvent, the mixture contains mainly the bad solvent (>98 vol%). The low concentration of the solute in that solution (typically less than 0.2 mM[21–23]) inevitably leads to unsatisfactory final crystal dimensions and limited coverage of crystals on the transistor substrates.[21,23] This restricts its practical applications in terms of efficiency and material usage.

In this study we describe a new method to grow single crystals of π-conjugated molecules from the solution phase, and its use in OFET device fabrication. In physical chemistry, the deviation from Raoult's law for non-ideal solvent combinations gives rise to azeotropism.[25] Its related phenomena of constant-boiling mixtures has long been studied in vapor–liquid equilibrium separation processes such as distillation.[26,27] Here, we adopt the

[*] X. Li, Prof. C. W. M. Bastiaansen, Prof. D. J. Broer
Department of Chemical Engineering and Chemistry
Eindhoven University of Technology
P. O. Box 513, 5600 MB Eindhoven (The Netherlands)
E-mail: X.Li@tue.nl
X. Li, Dr. G. H. Gelinck, Dr. B. K. C. Kjellander
Holst Centre
TNO-The Dutch Organization for Applied Scientific Research
High Tech Campus 31, 5656 AE Eindhoven (The Netherlands)
E-mail: gerwin.gelinck@tno.nl
Prof. J. E. Anthony
Department of Chemistry
University of Kentucky
Lexington, Kentucky 40506 (USA)
Prof. C. W. M. Bastiaansen
Queen Mary, University of London
Mile End Road, E1 4NS London (UK)
Prof. D. J. Broer
Philips Research Laboratories
Prof. Holstlaan 4, 5656 AE Eindhoven (The Netherlands)

concept of azeotropism to manipulate the morphology of deposited crystals, in an attempt to take advantage of the unique thermodynamics of azeotrope mixtures during evaporation.

Tri-isopropylsilylethynyl pentacene (TIPS-PEN) and its derivatives are among the most intensively studied soluble OSC because they combine high field-effect mobilities with good air stability.[28,29] Instead of transferring molecules from one solvent to another as in previous studies, we use stable binary solvent mixtures containing two solvents with opposing polarities. The two solvents are miscible and form a homogenous azeotrope mixture with a positive (low-boiling) azeotropic point. For such a system, the relative evaporation rate of the two solvents depends on the initial volume ratio. This allows us to control the late-stage composition of the solution during evaporation, and to study the effect thereof on the final morphology of TIPS-PEN. By studying different solvent compositions, we found a sharp transition in morphology, from polycrystalline-films to single crystals, at the azeotropic point. We also found that the morphology correlates well with transistor performance. Single crystal OFETs typically had a factor of 4 higher mobilities, with maximum values as high as $0.73 \, cm^2 \, V^{-1} \, s^{-1}$ in a bottom-contact device geometry. Moreover, the proposed method to manipulate crystal morphology can be extended to other π–π stacked organic molecules.

2. Results and Discussion

### 2.1. Azeotropic Mixture of Isopropanol/Toluene Binary Solvents

For this study we used a binary solvent system that comprises a polar (hydrophilic) solvent and an apolar (hydrophobic) one, for example, mixtures of isopropanol (IPA) plus toluene (Tol) with different IPA/Tol ratios (v/v). When these binary solvent mixtures evaporated on silicon wafers in ambient condition, the temporal change in solvent composition was studied using gas chromatography–mass spectrometry (GC–MS). From the results shown in Figure 1, it is clear that the relative evaporation rates of IPA and toluene depend on the initial solvent compositions. For binary mixtures with an IPA content of <50 vol%, IPA evaporates faster so that the mixture ends up with only toluene (Fig. 1, left). If the initial IPA content is above 50 vol%, however, IPA evaporates slower than toluene, and now the solvent mixture becomes more IPA-rich with time (Fig. 1, right). At a ratio ≈50/50 (v/v), the evaporation rate for

IPA and toluene is approximately the same, the vapor composition equals the composition of the liquid mixture remaining on the substrate, and the liquid composition maintains unaltered throughout drying (Fig. 1, middle). The measured composition change during evaporation is in good agreement with a previous report in which the refractive index of solvent mixtures was used to determine that IPA and toluene form a positive (low-boiling) azeotropic mixture at an IPA/Tol composition of 50.1/49.9 (v/v) at room temperature.[25,26]

2.2. Morphology Transition at Azeotropic Point & Single Crystal Formation

Based upon the azeotropic drying behavior of IPA/Tol mixtures, we make use of the late-stage composition of the binary solvents to manipulate the morphology of TIPS-PEN crystals. TIPS-PEN was dissolved in binary solvents of IPA/Tol with different IPA/Tol ratios (v/v). A few drops of each solution were placed on a silicon wafer in ambient atmosphere. Drying was completed in a few minutes. The resulting morphology was studied using cross-polarized optical microscopy (Fig. 2A). Dissolved in pure toluene, TIPS-PEN precipitated in the form of a polycrystalline film with small needles (Fig. 2A, 0/100). This morphology has, in fact, been reported by others.[30–32] With increasing IPA content, the film remained polycrystalline, but the polycrystallites became larger (Fig. 2A, 45/55). For IPA/Tol ratios greater than 50/50 (v/v), we observed discrete single crystals rather than films. This is illustrated by the micrograph of the 55/45 mixture in Figure 2A. The shape and size of the single crystals became more uniform, when the IPA content was increased up to 80 vol% (Fig. 2A, 80/20). We can now relate the abrupt change in crystal morphology to the final-state composition of the solvent mixture. As shown in Figure 2A, this transition occurs at the azeotropic point (50.1/49.9) between the 45/55 and 55/45 ratios of IPA/Tol (v/v). Replacing IPA with a less polar solvent, for example, ethanol (EtOH), which also forms a low-boiling azeotropic mixture when mixed with toluene at the composition of 59.8/40.2 (EtOH/Tol, v/v) at an ambient temperature of 25 °C,[26] the morphologies of TIPS-PEN drop-cast from EtOH/Tol mixtures showed the same transition at the azeotropic point from polycrystalline multi-domains (58/42) to single crystals (62/38), as depicted in Figure 2B.

To further elucidate the underlying principles for the formation of single crystals, we measured the UV–vis absorption spectra of
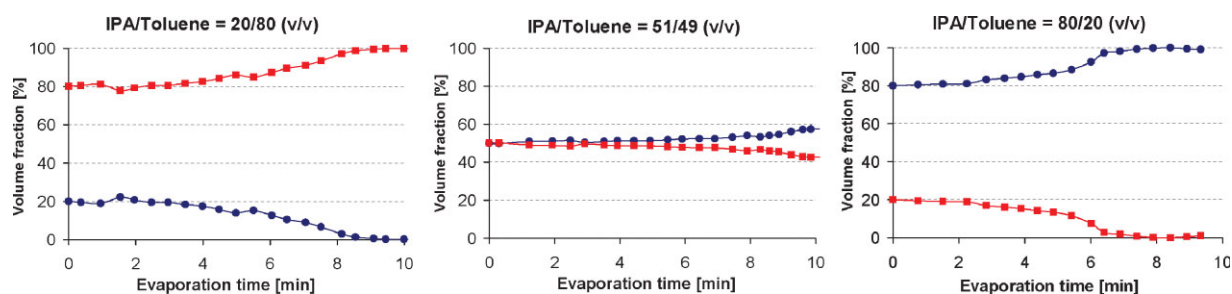
Figure 1. Change in solvent compositions during evaporation for three different IPA/Tol mixtures. Initial IPA/Tol volume ratios are indicated in the graph titles, from left to the right: 20/80; 51/49; and 80/20. Blue circles represent the volume fraction of IPA; red squares denote that of toluene.
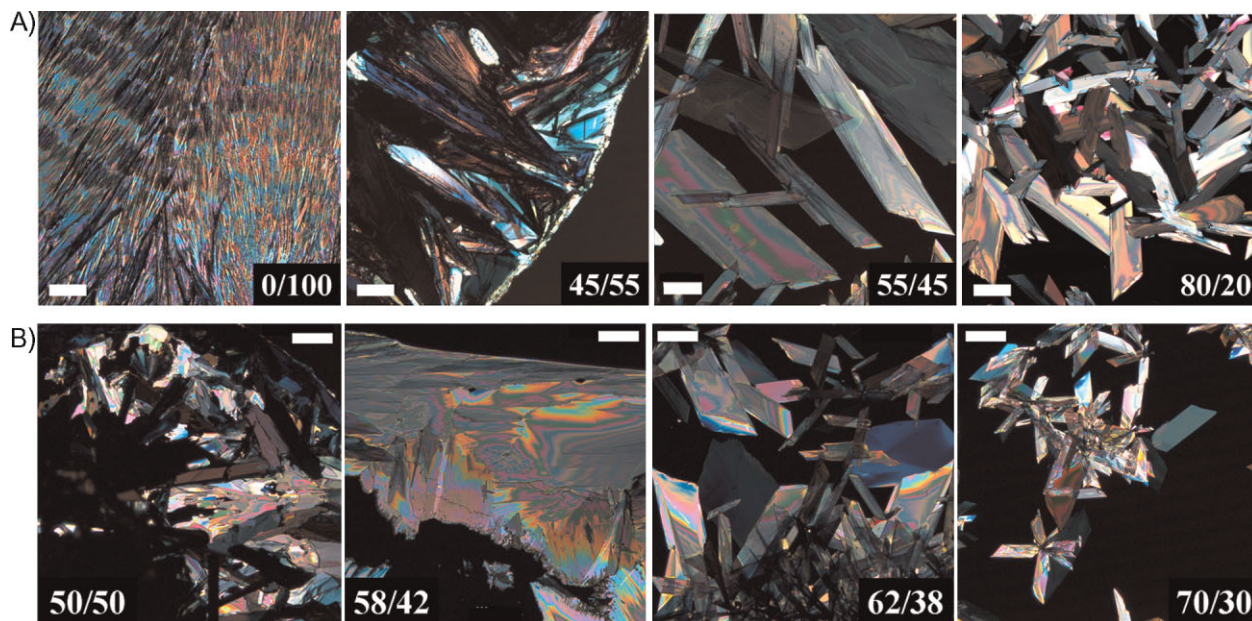
Figure 2. A) Representative cross-polarized optical micrographs showing an abrupt change of crystal morphology from polycrystalline domains (45/55) to large single crystals (55/45) with gradually increased volume ratios (v/v) of IPA in the binary solvent mixtures of IPA/Tol. In this range the azeotropic point of IPA/Tol is present at 50.1/49.9 (v/v). The volume fractions of IPA/Tol mixtures used for drop-casting are indicated at the right-bottom corner of each image (IPA/Tol, v/v). Scale bars represent 200 μm. B) Cross-polarized optical micrographs showing the morphology transition of TIPS-PEN crystals drop-cast on silicon wafers using EtOH/Tol mixtures with the volume fractions as indicated (EtOH/Tol, v/v). The azeotropic point of EtOH/Tol is at 59.8/40.2 (v/v). Scale bars represent 200 μm.

TIPS-PEN dissolved in IPA/Tol mixtures with different ratios (at a constant TIPS-PEN concentration). As shown in Figure 3A, a blueshift in absorption bands was observed with a gradual increase in IPA ratio. No spectral broadening was found. We also note that the spectra did not change with time, nor did we observe any precipitation of TIPS-PEN.

In a supramolecular aggregation of π-conjugated species, molecules can align in two (extreme) geometries: with the transition dipole moments of neighboring molecules "parallel" (H-aggregation) or "in-line" (J-aggregation).[33–36] Electronic interaction between the two transition dipole moments result in opposite spectral shifts: H-aggregates exhibit a blueshifted absorption band with respect to the absorption of isolated

molecules, while J-aggregates give a redshift.[37–40] A redshift would be expected with increased solvent polarity (more IPA ratio) if solvatochromic effects were dominant.[41] Therefore, the observed net effect of blueshifts here demonstrates that the TIPS-PEN molecules pack in supramolecular aggregates with parallel transition dipoles (H-aggregate) in IPA/Tol mixtures. This is in line with the reported "face-to-face (2D brick-wall)" structure of TIPS-PEN in the solid state, dominated by a co-facial π–π stacking of the acene backbones.[2,28,42] The presence of transition points at ~563 and 615 nm in Figure 3A (see Fig. S1, Supporting Information, for more details) indicates the stoichiometric conversion from individual molecules into H-aggregates with increased IPA/Tol ratios.

These progressively blueshifted absorption bands (Fig. 3A) suggest that a gradual elevation of the polar environment in solution induced by the hydroxyl group of IPA tends to facilitate the intermolecular overlapping of π orbitals between the intrinsically apolar pentacene backbones of TIPS-PEN, which has a symmetrical molecular configuration in a two-dimensional space, as shown in Figure 3B. Therefore, the tendency for individual TIPS-PEN molecules to associate into H-aggregates is substantially enhanced by adding more IPA to the solvent mixture, that is, the presence of the hydroxyl groups of IPA plays an important role in promoting such an aggregation. Since similar crystallochromy effect has already been well studied in perylenes and other
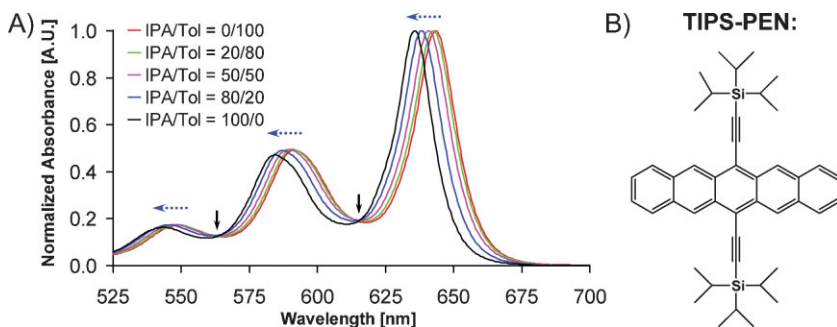
Figure 3. A) UV/Vis absorbance spectra of TIPS-PEN dissolved with different IPA/Tol solvent mixtures (and a constant concentration of 0.04 mg mL^{-1}). Dotted blue arrows illustrate the blueshifts with increased IPA/Tol ratios. Solid black arrows point at two transition points at ~563 and 615 nm, respectively. B) The chemical structure of a TIPS-PEN molecule.
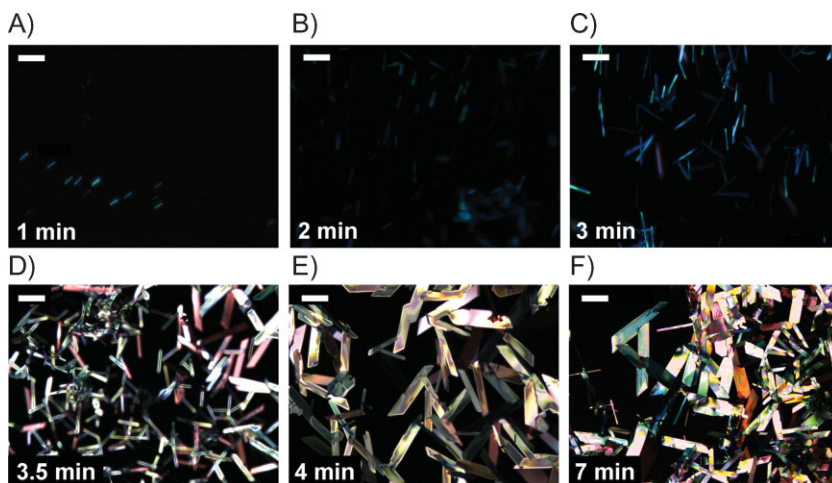
Figure 4. Time-resolved in situ observations for H-aggregate-induced crystallization of TIPS-PEN during the evaporation of binary solvent mixture (IPA/Tol: 80/20, v/v) on a silicon wafer under a cross-polarized microscope. All images were taken following the same spot on the liquid mixture and in the sequence of evaporation times upon drop-casting. The inset in the left bottom corner of each image indicates the evaporation time. Scale bars represent 200 μm.

seeding/nucleation sites for the crystallization from the bulk of the solution. As a result, single crystals grow and finally are deposited on the substrate (Fig. 2A: 55/45 and 80/20; Fig. 2B: 62/38 and 70/30). If, on the other hand, a mixture is drop-cast with a starting composition of alcohol below that of the azeotropic point, the solvent composition is getting richer in toluene while drying, and finally only toluene is left in the solvent so that TIPS-PEN solidifies at the contact line on the substrate in the form of thin-films or polycrystalline multidomains (Fig. 2A: 0/100 and 45/55; Fig. 2B: 50/50 and 58/42).

2.3. Characterizations of TIPS-PEN Single Crystals

As shown in Figure 5A, most of the TIPS-PEN single crystals grown with our method resemble parallelepipeds; a few appear like platelets. A side-view scanning electron microscopy (SEM) image (Fig. 5B) shows their well-defined crystal facets. The highly crystalline nature of the TIPS-PEN crystals was confirmed by X-ray measurements. The specular ($\theta/2\theta$ mode)

π-conjugated dye molecules,[43–46] a more quantitative analysis here is considered to be beyond the scope of the current study. We propose at this point that the supramolecular aggregates of TIPS-PEN act as initial seeding or nucleation sites for the single crystals that are formed during solvent evaporation.
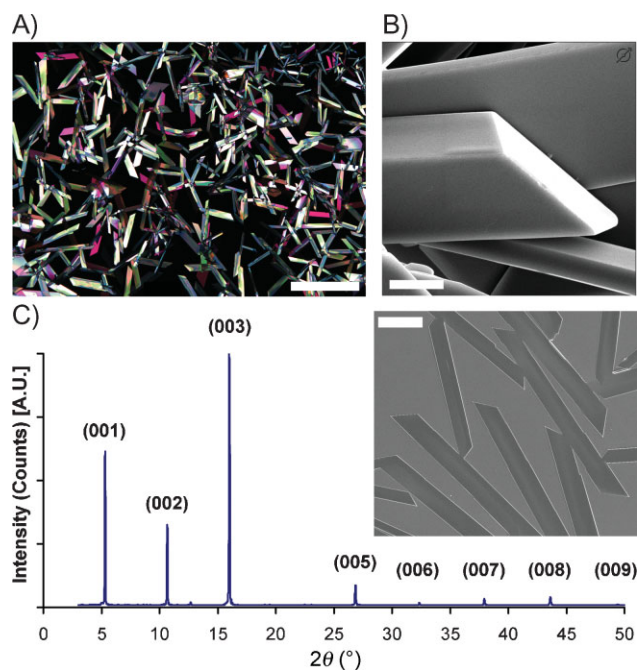
Furthermore, we studied the growth procedure of single crystals by using cross-polarized optical microscope. A binary solvent mixture of 2 mg TIPS-PEN per mL IPA/Tol (80/20, v/v) was drop-cast on a silicon wafer and observed in situ during solvent evaporation (Fig. 4A–F). After ∼1 minute of evaporation, small crystallites appeared in the solution (Fig. 4A). With time the crystals grew in size while floating (Fig. 4B–D). After ∼4 minutes the self-assembly of TIPS-PEN was almost complete (Fig. 4E), and no important changes were observed until the solvents were completely evaporated at ∼7 minutes (Fig. 4F). Note that the initial crystallites (Fig. 4A) emerged from the bulk of the solution rather than grafted from the surface of the substrate, thus no specific interaction with the substrate is involved during the growth of these single crystals. Interestingly, in the time-span from 3.5 to 4 minutes during crystal growth (from Fig. 4D to 4E), we observed a reduction in number of crystals as a result of "Ostwald ripening": it is thermodynamically more favorable to grow large crystals at the expense of small ones, due to the energetically more favorable volume to surface area ratio of bigger crystals.[47–51]

We can now rationalize the abrupt change in crystal morphology based on i) the azeotropic behavior of the solvent mixtures during evaporation, ii) the formation of H-aggregates in static binary solvents, and iii) the observation that the single crystals are formed in the bulk of the solution. Upon drop-casting TIPS-PEN in a binary solvent mixture at compositions of the polar component (alcohol) higher than that of the azeotropic point (e.g., IPA/Tol > 50.1/49.9, v/v), the gradual increase of the alcohol (hydroxyl group) ratio weakens the solute-solvent interactions, and favors aggregation of TIPS-PEN molecules. The aggregates act as

Figure 5. A) Cross-polarized optical micrograph showing the uniform-sized TIPS-PEN singe-crystals on a silicon wafer. Scale bar represents 400 μm. B) A side view SEM image showing the edges of a TIPS-PEN single crystal. Scale bar represents 2 μm. C) Specular X-ray diffraction patterns ($\theta/2\theta$ mode) for the TIPS-PEN crystals dispersed on a silicon substrate. The peaks are attributed to the (00l) lattice plane in the crystals. The inset is an SEM image showing a top-view of the uniform-dispersed single crystals used for XRD measurement. The scale bar in the inset image represents 100 μm. Part (C) of this figure was edited on 16.11.2009, after online publication, to include the x-axis label.

X-ray diffraction (XRD) pattern is shown in Figure 5C. The inset is a top-view SEM image of the uniform-dispersed single crystals on a silicon substrate used for the XRD measurement. The peak in Figure 5C at 5.3° (2θ) is attributed to the (001) reflection for the TIPS-PEN single crystal structure, as previously reported,[28,30] and corresponds to a lattice plane distance of 16.6 Å. This indicates that the TIPS-PEN molecules are oriented with the pentacene backbone parallel to the substrate surface. The other diffraction peaks in Figure 5C can all be attributed to higher-order reflections of the same lattice plane distance. In addition, several previous studies using electron diffraction pattern analysis have confirmed that TIPS-PEN crystals with regular sides (parallele-piped shape) and well-defined crystal facets are indeed single crystalline.[21,23,30]

The single crystals prepared using our approach have sizes as large as 2 mm × 0.7 mm. Their thickness is typically 0.5–2 μm. We found that the dimensions of the crystals increase with both the volume and concentration of the drop-cast solution, or, in other words, the total amount of TIPS-PEN molecules. The typical concentration used was 2–4 mg mL^{-1}. Because this is much higher than the concentration typically used in solvent-exchange method,[21–23] we obtained both larger crystals as well as higher surface coverage. Moreover, comparable with the tetracene single crystals prepared by physical vapor transport,[52] our relatively thin single crystals (with thickness below 1 μm) also displayed a potential mechanical flexibility. The SEM image in Figure S2 (Supporting Information) implies a good flexibility of the thin crystals: the long ribbon-like crystals (with thickness ≈500–600 nm) did not fracture even when they were bent at an angle of almost 180°.

2.4. Single Crystal OFETs & Correlation of Morphology with Mobility

TIPS-PEN solutions with 4 different ratios of IPA/Tol (0/100, 45/55, 55/45, and 80/20: v/v) were used to fabricate bottom-contact transis-tors. No apparent trend in transistor perfor-mance with solvent composition was found between the 0/100 and 45/55 mixtures, nor between the 55/45 and 80/20 mixtures. The mobility data in Figure 6A is therefore classified as either being from thin-film (for solvent compositions of 0/100 and 45/55) or single-crystal (55/45 and 80/20) transistors, depend-ing on whether the initial solvent ratio is below or above the azeotropic point of IPA/Tol. In total, 43 single-crystal OFETs in three different batches were measured. Only transistors with channel coverage of more than 30% were considered. Figure 6B depicts the transfer characteristics in both the linear and saturation regime for a group of 11 single-crystal transistors. Their gate-leakage current I_G is ~10^4 times lower than the source–drain current I_{DS}, and no hysteresis was observed during I–V dual scans.

The mobilities (μ) of transistors in the saturation regime were calculated from the equation as follows:[53]

$$\mu = \frac{2L}{WC_i} I_{DS}(V_G - V_{th})^{-2} \qquad (1)$$

where C_i is the capacitance per unit area of the gate dielectric layer, V_{th} is the threshold voltage, and L and W are the effective channel length and width, respectively, as estimated from the optical micrographs. The mobilities for 43 single-crystal transistors ranged from 0.03 to 0.73 cm^2 V^{-1} s^{-1} (Fig. 6A, left). Their average value was 0.18 cm^2 V^{-1} s^{-1}, and the standard deviation was 0.13 cm^2 V^{-1} s^{-1} (Fig. 6A, right). An average on/off ratio larger than 10^6 was obtained and most of these devices showed a V_{th} value close to zero. The near-zero threshold voltage is exceptionally low compared with other organic single crystal transistors,[13] and suggests a clean and good contact between the TIPS-PEN single crystals and the dielectric,[21] in line with the cross-section SEM image in Figure 6C. Such a good quality of semiconductor/dielectric interfaces in our bottom-contact single crystal transistors is most likely attributed to at least 3 factors: i) the flat surfaces of these highly crystalline TIPS-PEN crystals with well-defined crystal facets; ii) the unique thermodynamics of azeotrope mixtures during the last minute of solvent drying; iii) a good mechanical flexibility of the ribbon-like crystals (Fig. S2, Supporting Information). During the fabrication of our single crystal transistors, it is the low boiling point solvent IPA (b.p. = 82.3 °C) that remains on the transistor substrates at the final stage of solvent evaporation. Therefore, we believe the
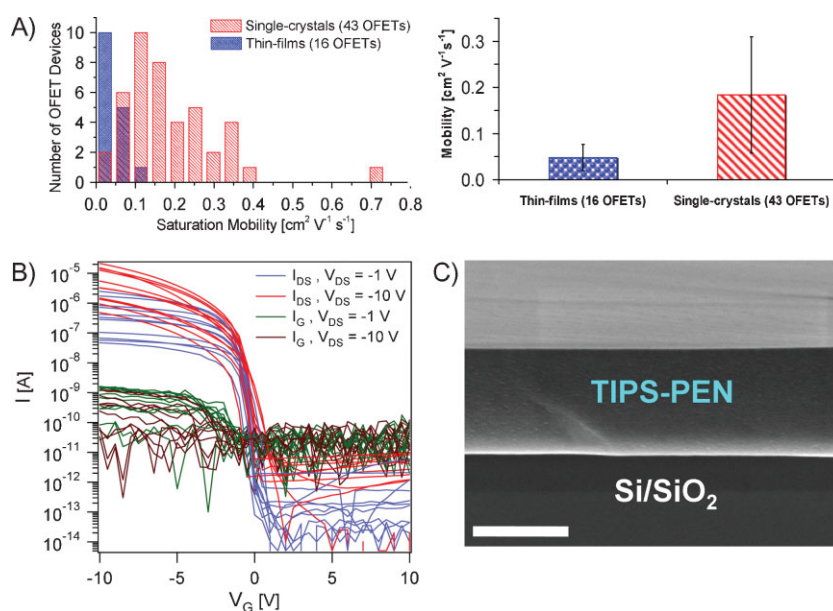
Figure 6. A) Transistor data of thin-film and single-crystal OFETs. Left: histograms of saturation mobilities of thin-film transistors (16 devices) and single crystal transistors (43 devices); right: average mobility and standard deviation (indicated by the bars) of thin-film and single crystal transistors. B) Transfer characteristics (linear and saturation regime) of 11 single crystal OFETs fabricated by using binary solvent mixture of IPA/Tol (80/20, v/v) under ambient clean room conditions. C) A representative cross-section SEM image showing an intimate contact between a TIPS-PEN single crystal and a SiO$_2$ dielectric layer. The scale bar represents 1 μm.

A)
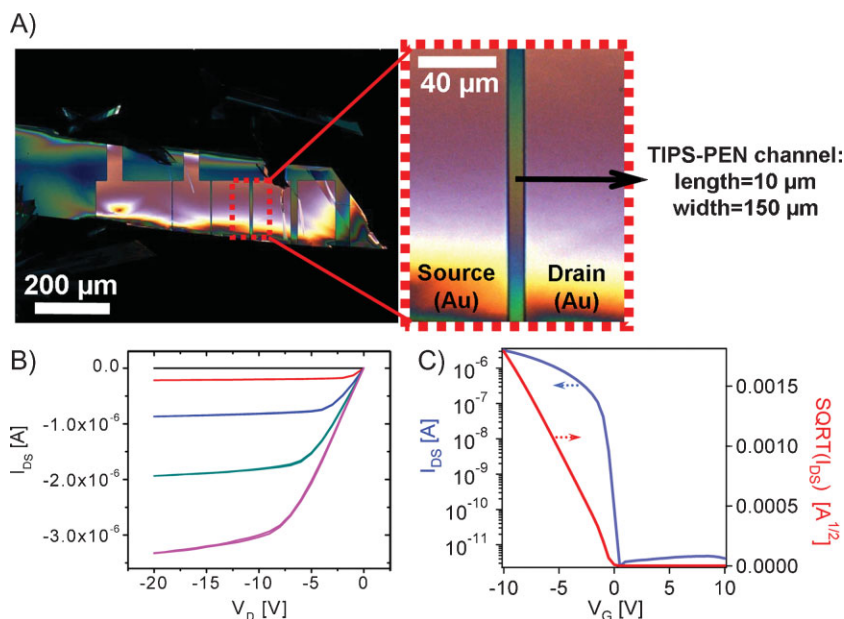
Figure 7. A) Left: cross-polarized optical micrograph of typical single crystal OFETs; right: a magnified image showing a transistor channel with channel length of 10 μm and width of 150 μm. B) Output characteristics and C) transfer characteristics ($V_{DS} = -10$ V) of the device shown in A. Curves of I_{DS} with different colors in B) correspond to different gate-bias (V_G): black = 0 V, red = −2.5 V, blue = −5 V, green = −7.5 V, and pink = −10 V, respectively.

capillary force driven by a very fast drying (outgoing) flow of the residual IPA beneath TIPS-PEN crystals tends to facilitate the formation of an intimate contact between the deposited single crystals and the transistor channels, assisted by the mechanical flexibility of the ribbon-like crystals.[52] Moreover, single crystal transistors fabricated under N_2 and ambient air exhibited very close average mobility values (0.17 and 0.19 cm^2 V^{-1} s^{-1}, respectively), illustrating the earlier reported air stability of TIPS-PEN.[32]

Figure 7 represents data of a typical single-crystal transistor. Figure 7A is a cross-polarized optical micrograph. The zoomed-in image on the right depicts the transistor channel with an effective width (W) of 150 μm and length (L) of 10 μm. The field-effect performance of this device is plotted in Figure 7B and C as its output and transfer characteristics, respectively. No contact resistance was observed from the output characteristics, which implies a good electrical contact between the crystals and bottom Au electrodes. The mobility (μ) of this particular OFET in the saturation regime was calculated to be 0.39 cm^2 V^{-1} s^{-1}, and a near-zero threshold voltage (V_{th}) of −0.15 V for this device was extracted by extrapolating the square root (SQRT) of $|I_{DS,sat}|$ versus V_G plot to $I_{DS,sat} = 0$ (this value was changed from 0, 0 on 16.11.2009, after online publication), as depicted in the red curve in Figure 7C.

The morphology of OSC is one of the dominating factors for its electronic performance.[2,9,12,30] We also found a clear correla-

tion between the morphology category (thin films or single crystals) and the field-effect mobility of the transistors. The mobility of the single crystal transistors was a factor of ∼4 higher, which is close to a previously reported value of ∼4.4.[21] Other transistor parameters such as threshold voltage were independent of the morphology. For both groups of devices (thin films and single crystals), the range in mobility was rather broad (Fig. 6A, left). We note that this relatively large spread is in fact expected, since the crystal orientation with respect to the transistor channel direction is not controlled and the charge transport in this material is dependent on the crystallographic direction.[54] However, the spread can not only be attributed to the intrinsic anisotropy of charge-transport in single crystals; variations of the crystal quality and/or the contact of the crystals with Au bottom electrodes can also be of importance, as suggested elsewhere.[55]

2.5. Applicability to other π–π Stacked Molecules

In light of the single-crystal formation of TIPS-PEN, we chose two other π-conjugated molecules and studied their crystal formation by using azeotropic binary solvent mixtures. A soluble acene-based OSC, fluorinated 5,11-bis(triethylsilylethynyl) anthradithiophene (diF-TES ADT),[8,56] and a widely-used derivative of naphthalene, 2-phenylnaphthalene,[57] were drop-cast from either a single good solvent (toluene) or a binary solvent of IPA/Tol with an initial composition above the azeotropic point. We also
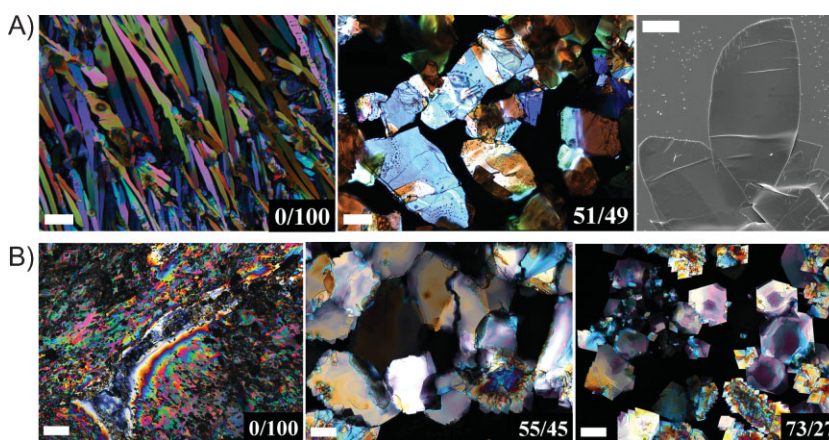
Figure 8. Cross-polarized optical micrographs showing the morphology transition of diF-TES ADT and 2-phenylnaphthalene, respectively, by drop-casting from a single good solvent (toluene) or a binary solvent of IPA/Tol with an initial composition above their azeotropic point. The volume fractions of IPA/Tol mixtures used are indicated at the right-bottom corner of each optical micrograph (IPA/Tol, v/v). A) diF-TES ADT: morphology change from small needles (0/100) to individual big platelets (51/49). On the right is a top-view SEM image showing a representative platelet, its scale bar is 50 μm. B) 2-phenylnaphthalene: morphology transitions from thin-film domains (0/100) to big platelets (55/45), then to rectangle or hexagon-shaped crystals (73/27). Scale bars in all optical micrographs represent 100 μm.

found a morphology transition from polycrystalline thin-film domains to individual large crystals (Fig. 8). The change in morphology of these two molecules at the azeotropic point of IPA/Tol mixtures is in line with that of TIPS-PEN.

The morphology transitions presented in Figure 8, together with the results of TIPS-PEN, suggest a broad applicability of using azeotropic binary solvent system to manipulate the crystal morphology for conjugated molecules with strong π–π intermolecular interactions (effective overlap of the π orbitals). Functionalized acenes with close cofacial face-to-face arrangement of the acene backbones are among this group of molecules. In general, these aromatic molecules have a sufficient solubility in hydrophobic (apolar) solvents and a very poor solubility in hydrophilic (polar) solvents. Such considerable difference in solubility allows us to obtain the desirable crystal morphology through controlling the late-stage solvent composition of azeotrope mixtures via adjusting their initial ratio. TIPS-PEN is an excellent study module for our proposed method, thanks to its conformational flexibility of the triisopropylsilyl side group which gives it sufficient solubility in apolar solvents, and an increased density of its bulky groups which enables the tight packing of the pentacene backbones to maximize their π–π interactions.[21]

3. Conclusions

In conclusion, this study describes a new approach to form single crystals of π–π stacked organic molecules by using azeotropic binary solvent mixtures. Large crystals (length and width of up to 2 millimeters and 700 μm, respectively) of tri-isopropylsilylethynyl pentacene with predominately parallelepiped shape are facilely self-assembled in a well-controlled manner. Based on the concept of azeotropism and the different solubility of TIPS-PEN in polar or apolar solvents, the size and shape of the crystals can be manipulated from small needles to large parallelepipeds, via adjusting the initial ratio (v/v) of the two components in our binary solvent system with respect to their azeotropic point. We explain the formation mechanism of large single crystals: during the evaporation of azeotrope mixtures, the change in solvent composition promotes an efficient nucleation from the H-aggregates of TIPS-PEN, and facilitates a fast crystallization thereof. Meanwhile, a broader applicability of our method to other π–π stacked organic molecules is demonstrated. When used as active layer in bottom-contact field-effect transistors, the TIPS-PEN single crystals exhibit an enhanced charge transport properties compared to transistors with polycrystalline-films. Additionally, a higher efficiency for the fabrication of single crystal transistors, a better crystal coverage on device substrates, and an improved semiconductor/dielectric interface are obtained.

The promising technological applications of organic semiconductors will benefit from the development of efficient, inexpensive, and easily controlled deposition methods. Direct deposition of organic single crystals from the solution phase offers an elegant and effective route. The new method described here provides a general and rational approach to the formation of large single crystals of π-conjugated organic molecules from solution. Its broad applicability appears to be of interest for certain exploratory research and potential applications in materials science, for which simplicity, rationality, and processing efficiency are the main advantages.

4. Experimental

Tri-isopropylsilylethynyl pentacene (TIPS-PEN) [28,58] and fluorinated 5,11-bis(triethylsilylethynyl) anthradithiophene (diF-TES ADT) [59] were synthesized according to the procedures reported earlier. 2-phenylnaphthalene was purchased from ABCR GmbH & Co. KG (Germany). All solvents were used as received without further treatments. Toluene (analysis grade) was purchased from Merck. Isopropanol (laboratory reagent grade) and ethanol (absolute) were purchased from Fisher Scientific and BASF, respectively. All experiments were conducted at room temperature. TIPS-PEN solutions with different solvent ratios were prepared prior to drop-casting. Drop-casting was carried out in an ambient clean room environment or under N_2 atmosphere. Gas chromatography-mass spectrometry was done using an Agilent 6890GC with a 5973MSD. Measurements were performed by applying 10 droplets of the mixture onto a silicon wafer; a small volume was taken from the remainder liquid mixture in the sequence of evaporation times and immediately injected into the GC-MS setup. UV/Vis absorption spectra were recorded on a Shimadzu UV-3102PC UV-VIS-NIR scanning spectrophotometer. Optical micrographs were taken by using a Leica DM2500 M Microscope with cross polarizers. SEM images were obtained on an FEI Quanta 3D FEG field-emission scanning electron microscope. XRD measurements were performed in the specular reflection mode ($\theta/2\theta$) at 40 kV and 30 mA with a Cu Kα1 radiation using a Rigaku X-ray diffractometer. Bottom-contact/bottom-gate transistors were fabricated on Si (n++)/SiO$_2$ substrates with photolithographically patterned Au as source and drain electrodes. A pentafluorobenzenethiol monolayer was deposited on Au electrodes to lower the contact resistance [29,60]. The SiO$_2$ was treated with trichlorophenylsilane to improve the wetting [61]. An HP Agilent 4155C semiconductor parameter analyzer was used to measure the electrical characteristics of OFETs (current-voltage scans) under N_2 atmosphere in a glove-box.

[1] N. Stingelin-Stutzmann, *Nat. Mater.* **2008**, *7*, 171.

[2] J. A. Lim, H. S. Lee, W. H. Lee, K. Cho, *Adv. Funct. Mater.* **2009**, *19*, 1515.

[3] D. Braga, G. Horowitz, *Adv. Mater.* **2009**, *21*, 1473.

[4] S. Liu, W. M. Wang, A. L. Briseno, S. C. B. Mannsfeld, Z. Bao, *Adv. Mater.* **2009**, *21*, 1217.

[5] H. E. A. Huitema, G. H. Gelinck, J. B. P. H. van der Putten, K. E. Kuijk, C. M. Hart, E. Cantatore, P. T. Herwig, A. J. J. M. van Breemen, D. M. de Leeuw, *Nature* **2001**, *414*, 599.

[6] E. Cantatore, T. C. T. Geuns, G. H. Gelinck, E. van Veenendaal, A. F. A. Gruijthuijsen, L. Schrijnemakers, S. Drews, D. M. de Leeuw, *IEEE J. Solid-State Circuits* **2007**, *42*, 84.

ADVANCED FUNCTIONAL MATERIALS

FULL PAPER

[7] C. S. Kim, S. Lee, E. D. Gomez, J. E. Anthony, Y. Loo, *Appl. Phys. Lett.* **2008**, *93*, 103302.

[8] D. J. Gundlach, J. E. Royer, S. K. Park, S. Subramanian, O. D. Jurchescu, B. H. Hamadani, A. J. Moad, R. J. Kline, L. C. Teague, O. Kirillov, C. A. Richter, J. G. Kushmerick, L. J. Richter, S. R. Parkin, T. N. Jackson, J. E. Anthony, *Nat. Mater.* **2008**, *7*, 216.

[9] S. K. Park, T. N. Jackson, J. E. Anthony, D. A. Mourey, *Appl. Phys. Lett.* **2007**, *91*, 063514.

[10] N. Liu, Y. Zhou, L. Wang, J. Peng, J. Wang, J. Pei, Y. Cao, *Langmuir* **2009**, *25*, 665.

[11] J. A. Lim, W. H. Lee, H. S. Lee, J. H. Lee, Y. D. Park, K. Cho, *Adv. Funct. Mater.* **2008**, *18*, 229.

[12] I. Mcculloch, *Nat. Mater.* **2005**, *4*, 583.

[13] Q. Tang, L. Jiang, Y. Tong, H. Li, Y. Liu, Z. Wang, W. Hu, Y. Liu, D. Zhu, *Adv. Mater.* **2008**, *20*, 2947.

[14] A. L. Briseno, S. C. Mannsfeld, S. A. Jenekhe, Z. Bao, Y. Xia, *Mater. Today* **2008**, *11*, 38.

[15] C. Reese, Z. Bao, *Mater. Today* **2007**, *10*, 20.

[16] A. Molinari, I. Gutierrez, I. N. Hulea, S. Russo, A. F. Morpurgo, *Appl. Phys. Lett.* **2007**, *90*, 212103.

[17] E. Menard, A. Marchenko, V. Podzorov, M. E. Gershenson, D. Fichou, J. A. Rogers, *Adv. Mater.* **2006**, *18*, 1552.

[18] Y. Sun, L. Tan, S. Jiang, H. Qian, Z. Wang, D. Yan, C. Di, Y. Wang, W. Wu, G. Yu, S. Yan, C. Wang, W. Hu, Y. Liu, D. Zhu, *J. Am. Chem. Soc.* **2007**, *129*, 1882.

[19] V. Y. Butko, X. Chi, D. V. Lang, A. P. Ramirez, *Appl. Phys. Lett.* **2003**, *83*, 4773.

[20] A. S. Molinari, H. Alves, Z. Chen, A. Facchetti, A. F. Morpurgo, *J. Am. Chem. Soc.* **2009**, *131*, 2462.

[21] D. H. Kim, D. Y. Lee, H. S. Lee, W. H. Lee, Y. H. Kim, J. I. Han, K. Cho, *Adv. Mater.* **2007**, *19*, 678.

[22] K. Balakrishnan, A. Datar, R. Oitker, H. Chen, J. Zuo, L. Zang, *J. Am. Chem. Soc.* **2005**, *127*, 10496.

[23] S. J. Kang, I. Bae, Y. J. Park, T. H. Park, J. Sung, S. C. Yoon, K. H. Kim, D. H. Choi, C. Park, *Adv. Funct. Mater.* **2009**, *19*, 1609.

[24] S. J. Kang, Y. J. Park, I. Bae, K. J. Kim, H. Kim, S. Bauer, E. L. Thomas, C. Park, *Adv. Funct. Mater.* **2009**, *19*, 2812.

[25] P. W. Atkins, in *Physical Chemistry*, 5th ed. Oxford University Press, Oxford, UK **1994**, p. 245.

[26] E. Robinson, W. A. Wright, G. W. Bennett, *J. Phys. Chem.* **1932**, *36*, 658.

[27] J. Gmehling, J. Menke, J. Krafczyk, in *Azeotropic Data*, Vol. *1*, 2nd ed. Wiley-VCH, Weinheim, Germany **2004**.

[28] J. E. Anthony, J. S. Brooks, D. L. Eaton, S. R. Parkin, *J. Am. Chem. Soc.* **2001**, *123*, 9482.

[29] M. M. Payne, S. R. Parkin, J. E. Anthony, C. C. Kuo, T. N. Jackson, *J. Am. Chem. Soc.* **2005**, *127*, 4986.

[30] J. H. Chen, D. C. Martin, J. E. Anthony, *J. Mater. Res.* **2007**, *22*, 1701.

[31] J. H. Chen, S. Subramanian, S. R. Parkin, M. Siegler, K. Gallup, C. Haughn, D. C. Martin, J. E. Anthony, *J. Mater. Chem.* **2008**, *18*, 1961.

[32] S. K. Park, D. A. Mourey, J. Han, J. E. Anthony, T. N. Jackson, *Org. Electron.* **2009**, *10*, 486.

[33] M. Pope, C. E. Swenberg, in *Electronic Processes in Organic Crystals and Polymers, Part I: Optical Properties of Organic Molecules and Crystals*, 2nd ed. Oxford University Press, New York, USA, **1999**.

[34] E. G. McRae, M. Kasha, *J. Chem. Phys.* **1958**, *28*, 721.

[35] M. Kasha, H. R. Rawls, M. A. El-Bayoumi, *Pure Appl. Chem.* **1965**, *11*, 371.

[36] J. B. Birks, *Rep. Prog. Phys.* **1975**, *38*, 903.

[37] B. S. Ong, Y. Wu, P. Liu, *Proc. IEEE* **2005**, *93*, 1412.

[38] K. Takazawa, Y. Kitahama, Y. Kimura, G. Kido, *Nano Lett.* **2005**, *5*, 1293.

[39] G. Berkovic, V. Krongauz, V. Weiss, *Chem. Rev.* **2000**, *100*, 1741.

[40] B. K. An, D. S. Lee, J. S. Lee, Y. S. Park, H. S. Song, S. Y. Park, *J. Am. Chem. Soc.* **2004**, *126*, 10232.

[41] D. A. Skoog, J. J. Leary, in *Principles of Instrumental Analysis*, 4th ed. Saunders College Publishing, Philadelphia, USA **1992**, p. 153.

[42] F. A. Hegmann, R. R. Tykwinski, K. P. H. Lui, J. E. Bullock, J. E. Anthony, *Phys. Rev. Lett.* **2002**, *89*, 227403.

[43] P. M. Kazmaier, R. Hoffmann, *J. Am. Chem. Soc.* **1994**, *116*, 9684.

[44] G. Klebe, F. Graser, E. Hädicke, J. Berndt, *Acta Crystallogr. Sect. B* **1989**, *45*, 69.

[45] O. Valdes-Aguilera, D. C. Neckers, *Acc. Chem. Res.* **1989**, *22*, 171.

[46] C. A. Hunter, J. K. M. Sanders, A. J. Stone, *Chem. Phys.* **1989**, *133*, 395.

[47] J. D. Ng, B. Lorber, J. Witz, A. Theobald-Dietrich, R. Kern, R. Giege, *J. Cryst. Growth* **1996**, *168*, 50.

[48] R. Boistelle, J. P. Astier, *J. Cryst. Growth* **1988**, *90*, 14.

[49] A. Kabalnov, *J. Dispersion Sci. Technol.* **2001**, *22*, 1.

[50] T. Kraska, *J. Phys. Chem. B* **2008**, *112*, 12408.

[51] P. Taylor, *Adv. Colloid Interface Sci.* **2003**, *106*, 261.

[52] R. W. I. de Boer, T. M. Klapwijk, A. F. Morpurgo, *Appl. Phys. Lett.* **2003**, *83*, 4345.

[53] G. Horowitz, *Adv. Mater.* **1998**, *10*, 365.

[54] O. Ostroverkhova, D. G. Cooke, F. A. Hegmann, R. R. Tykwinski, S. R. Parkin, J. E. Anthony, *Appl. Phys. Lett.* **2006**, *89*, 192113.

[55] M. Mas-Torrent, M. Durkut, P. Hadley, X. Ribas, C. Rovira, *J. Am. Chem. Soc.* **2004**, *126*, 984.

[56] O. D. Jurchescu, S. Subramanian, R. J. Kline, S. D. Hudson, J. E. Anthony, T. N. Jackson, D. J. Gundlach, *Chem. Mater.* **2008**, *20*, 6733.

[57] H. E. Holloway, R. V. Nauman, J. H. Wharton, *J. Phys. Chem.* **1968**, *72*, 4474.

[58] J. E. Anthony, D. L. Eaton, S. R. Parkin, *Org. Lett.* **2002**, *4*, 15.

[59] S. Subramanian, S. K. Park, S. R. Parkin, V. Podzorov, T. N. Jackson, J. E. Anthony, *J. Am. Chem. Soc.* **2008**, *130*, 2706.

[60] D. J. Gundlach, L. L. Jia, T. N. Jackson, *IEEE Electron Device Lett.* **2001**, *22*, 571.

[61] D. Kumaki, M. Yahiro, Y. Inoue, S. Tokito, *Appl. Phys. Lett.* **2007**, *90*, 133511.

WILEY InterScience®
DISCOVER SOMETHING GREAT